Advances in Pulsed-Power-Driven Radiography Systems

John Maenchen, Steve Cordova, Fawn Griffin, Kelly Hahn, Deanna Jaramillo, Isidro Molina, Salvador Portillo, Elizabeth Puetz, Dean Rovang, Matt Scieford, Vernon Bailey[a], David L. Johnson[a], Ian Smith[a], Steve Swanekamp[a], Frank Young[a], David Van De Valde[b], Bryan Oliver[c], David Rose[c], Dale Welch[c], Gerald Cooperstein[c], Robert Commisso[d], David Hinshelwood[c], Dennis Barker[e], Darryl Droemer[e], Ray Gignac[e], Frank Wilkins[e], Bradley Shelton[f], John O'Malley[g], Ian Crotch[g], Ken Thomas[g], Jim Threadgold[g], Graham Cooper[g], and Mark Sinclair[g]

Sandia National Laboratorie, P.O. Box 5800, MS-1193, Albuquerque, New Mexico, 87185, USA, 505-845-8963, 505-844-8467, Maenchen@sandia.gov*
[a]Titan Pulsed Sciences Division, 2700 Merced Street, San Leandro, California, 94577 USA
[b]EG&G, PO Box 9100, Albuquerque, New Mexico, 87119, USA
[c]Mission Research Corporation, 5100 Indian School Road NE, Albuquerque, New Mexico, 87110, USA
[d]Naval Research Laboratory, Code 6770, 4560 Overlook Ave SW, Washington DC, 20375, USA
[e]Bechtel Nevada Corporation, 2621 Losee Road, North Las Vegas, Nevada, 89030, USA
[f]Ktech Corporation, 1300 Eubank SE, Albuquerque, New Mexico, 87123, USA
[g]Atomic Weapons Establishment, Aldermasten, Reading, RG7 4PR, United Kingdom

Abstract – Flash x-ray radiography has undergone a transformation in recent years with the resurgence of interest in compact, high intensity pulsed-power-driven electron beam sources. The radiographic requirements and the choice of a consistent x-ray source determine the accelerator parameters, which can be met by demonstrated Induction Voltage Adder technologies. This paper reviews the state of the art and the recent advances which have improved performance by over an order of magnitude in beam brightness and radiographic utility.

1. Introduction

The ability to drive various impedance focused electron beam diode loads with an Induction Voltage Adder (IVA) architecture is a recent area of research in pulsed-power-driven radiography. This application requires the generation of high current (30–100 kA) and high voltage (2–16 MV) electron beams. The different current-voltage operating points are driven by the radiographic needs for dose and spot and require different impedance diodes to span the breadth of requirements. For example, the rod-pinch diode is nominally a 45-Ohm source whereas the paraxial diode is a 200-Ohm source at 8 MV. A flexible accelerator that can efficiently drive either low or high impedance loads is attractive.

Section 2 will describe the focused electron beam diode loads suitable for flash radiography. Section 3 will briefly summarize the Induction Voltage Adder (IVA) accelerator architecture. Section 4 will present recent research on the design of both high and low impedance IVA's. Critical to the discussion is the operating point of the magnetically insulated vacuum transmission line (MITL), which threads the multiple induction cavities of a single IVA. Because the MITL operating impedance is non-linear and dependent upon the load impedance, it is possible to design flexibility into both the endpoint voltage and/or current of the accelerator either by modifying the dimensions of the MITL or changing the load impedance. Section 5 will present an approach to utilize these MITL operational features to use a single IVA accelerator to drive a variety of radiographic loads. Section 6 will summarize the results and provides suggestions for future improvements.

2. Radiographic Diodes

Pulsed-power-driven flash x-ray radiographic diodes have been used for decades to interrogate the interior mass distributions of dynamic experiments [1, 2]. The wide variety of possible objects requires a suite of radiographic source (driver and diode) capabilities, with metrics of beam brightness (hence resultant x-ray source intensity), focal spot diameter, and ease and reliability of operation. Recent research has improved our understanding of these flash radiographic sources and provided new levels of capability.

For all radiographic diodes considered here the x-ray source is produced by stopping a high-intensity pulsed electron beam in a high-atomic-number bremsstrahlung converter anode, producing a dose

* Sandia is a multiprogram laboratory operated by Sandia Corporation, a Lockheed Martin Company, for the United States Department of Energy's National Nuclear Security Administration under contract DE-AC04-94AL85000.

$$\frac{\text{rads}}{\text{Coulomb}} \approx 1290 V^{2.8} \exp\left[-\frac{(V+0.5)\beta_{\perp}}{0.67\pi}\right]$$

measured a meter from the source, where V is the applied voltage in megavolts and $\beta_{\perp}$ is the electron beam relativistic velocity component transverse to the radiographic axis. This scaling shows the tradeoff between voltage, current, and beam orientation.

The radiographic diodes are all designed for pulse durations of about 50 ns. Neither pulse shape nor flatness of the peak voltage is critical; a short rise time is desirable to maximize dose within the allowed pulse duration or diode impedance lifetime. For most diode designs, the accelerator "prepulse" that precedes the drive pulse can affect the diode performance duration.

Figure 1 shows a conventional industrial x-ray source where electrons are drawn from a cylindrical cathode inward toward a positively-biased conical anode. These diodes are operated at very high impedance (low current) and the anode deposition heating is kept below melt, allowing reliable multiple-shot operation at correspondingly low x-ray intensities. The radiographic axis is typically orthogonal to the electron orbits, acceptable at low (~ MV) voltages where the bremsstrahlung output is nearly isotropic. This diode can be designed with electrostatic tools, although use of electrodynamic codes can suggest modifications to significantly improve performance.

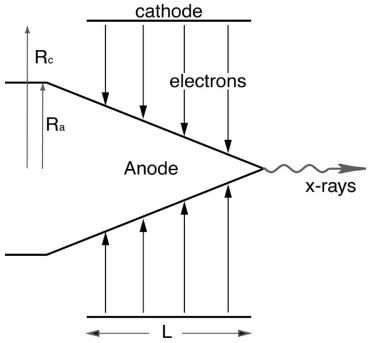

Fig. 1. Industrial x-ray source

Figure 2 shows a high current modification of this diode, called the rod pinch. The electron current is allowed to exceed the critical pinch current.

$$I_{\text{crit}}\,(\text{kA}) = 17(\gamma^2 - 1)^{1/2} / \ln(R_c / R_a)$$

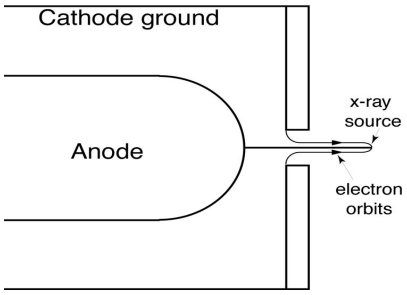

Fig. 2. Rod-pinch diode

Electron impact heating creates an anode plasma along the rod length. The released ions enable the electron flow to pinch, insulate and propagate along the rod to form a high intensity focal spot at the end [3, 4]. The rod-pinch diode is easy to assemble and align, reliably providing the smallest spot size (1 to 2 mm) of the high intensity sources to date [5]. The radiographic axis is again orthogonal to the final electron path, similarly restricting this diode to low voltage efficient operation. The rod-pinch is easy to understand in concept but is subtle to optimize and requires sophisticated hybrid (particle-in-cell with Monte Carlo combined with fluid) codes for accurate modeling [6, 7].

Figure 3 shows a negative polarity version of the pinching diode, called the self-pinch. Again the electron heating creates an anode plasma, releasing ions, which enable the formation of a high intensity electron pinch on axis. The electron orbits are now more closely aligned with the radiographic axis, thereby producing significantly more useful dose at multi-megavolt potentials. The pinch is self-generated and can wander, producing a larger time-integrated radiographic spot [8]. The cathode is highly enhanced and the pinching is self-initiated, making this diode very sensitive to prepulse and assembly procedures. Detailed modeling again requires hybrid codes.

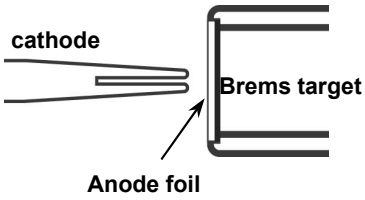

Fig. 3. Self-pinch radiographic diode

A concept, which combines the self-pinch and rod-pinch diodes, is shown in Fig. 4 [7] where computations suggest the self-pinch may stabilize under certain conditions on an extruded axial rod. This concept is now being evaluated experimentally.

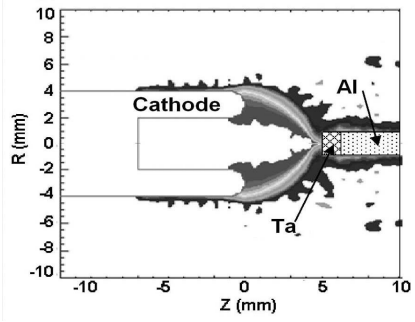

Fig. 4. Stabilized hybrid pinch diode concept

Figure 5 shows the paraxial diode, which has been used for thirty years to produce reliable TW/cm^2 focal spots on a variety of systems from 2 to 10 MV [1].

A cold electron beam is drawn from a spherical cathode and allowed to expand as it accelerates to ground.

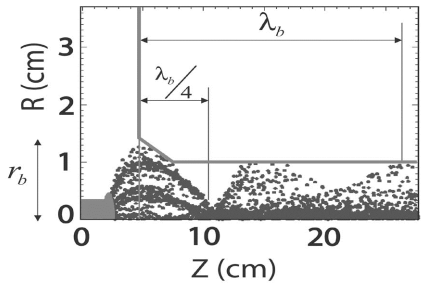

Fig. 5. Paraxial radiographic diode with betatron focusing

It passes through an anode foil at an intensity below that required to release ions [9] and enters a gas-filled transport cell. The gas ionizes through a variety of processes and focuses the electron beam onto the converter plane [10]. Electrons travel along the radiographic axis, producing a large useful dose. The vacuum region of the diode may be designed with electrostatic tools, but the gas transport remains difficult to model with today's computational codes. The focusing mechanism is chromatic and time dependent, due to net current evolution in the transport region, leading to a varying focal length and a larger, although very reliable, time-integrated radiographic spot. Investigations are underway to replace the gas fill with a pre-formed plasma to minimize net currents and beam sweeping and create a higher intensity reliable x-ray source.

Figure 6 shows a magnetically immersed radiographic source where the electron beam is emitted from a small cathode needle and transported to the anode converter in a strong solenoidal applied magnetic field [11].

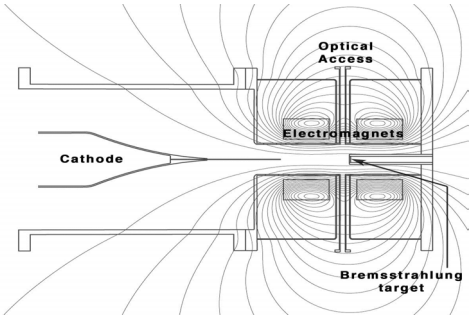

Fig. 6. Magnetically immersed diode

The current is limited by the electron beam (radius r_b) space charge within the cylindrical anode (radius R_w) to be

$$I_{\text{beam}} = \frac{17\,\text{kA}\left[\left(1+\frac{V}{511\,\text{kV}}\right)\right]}{\left(1-\frac{Zn_i}{n_e}\right)\left(1+2\ln\left(R_w/r_b\right)\right)}.$$

This source has demonstrated few-mm-diameter radiographic spots from 3 to 9 MV, operating at 10 TW/cm^2, and is under continued development to reduce the spot size while maintaining impedance stability. The electron beam is aligned with the radiographic axis, efficiently producing usable dose. Investigations of plasma formation and evolution, and approaches to control ion production are underway. The pulsed electromagnet increases the complication of using this source for radiographic applications compared to the alternatives described above, but offers a further control on performance stability at high voltages.

These radiographic diodes may be characterized by their impedance and radiation producing capabilities. Fig. 7 shows diode scaling relationships and the accelerators used to test them. Note the significant variation among radiographic diode impedances, compounded by the requirement to drive these devices with cathode conduction current from the high voltage vacuum feed (described below).

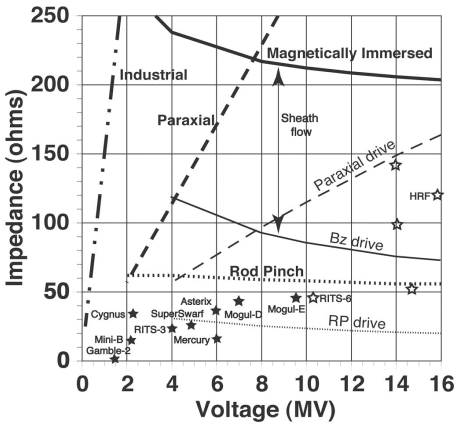

Fig. 7. Radiographic diode load lines. Operating (solid) and possible future (hollow) accelerators are shown

3. Induction Voltage Adder systems

Induction Voltage Adder accelerators were developed to exchange the difficulty of high voltage pulse formation and switching with the complexity of adding multiple synchronous lower-voltage modules [12–15]. The Radiographic Integrated Test Stand (RITS) (Fig. 8) at Sandia National Laboratories provides a worked example of an Induction Voltage Adder (IVA) accelerator. A 3-MV Marx generator pulse charges a water-dielectric coaxial capacitor in 800 ns, which is command-switched to pulse charge three 8-Ohm water coaxial pulse forming lines (PFLs) in about 200 ns. Each PFL charges as a capacitor but discharges as a transmission line, generating a double-transit duration square output pulse. Two successive stages of switched PFLs sharpen this pulse to a 10-ns rise time and reduce the series-capacitance prepulse to about a kilovolt. Each pulse compression line feeds an induction cavity (Fig. 8c) where current flow along the ground-side path is inhibited by use of a saturable

ferromagnetic for the pulse duration. The cavities are threaded by a central vacuum coax – effectively linking the pulse compression lines as parallel primaries to a common secondary in a transformer. The voltage appearing on this vacuum output transmission line is a wave phenomena, as the center conductor is cantilevered off ground while a multi-megavolt potential is applied to the load end.

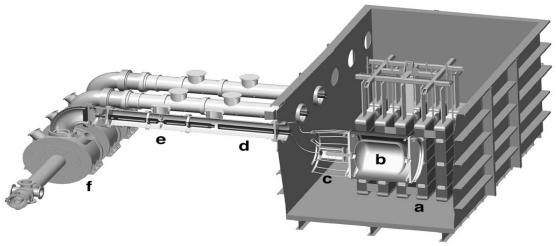

Fig. 8a. RITS: IVA accelerator (a), marx generator (b), transfer capacitor (c), gas switch (d), pulse forming line (e), peaking lines (f), induction cavities

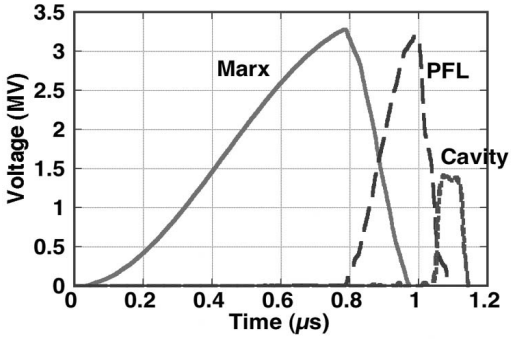

Fig. 8b. RITS Pulse waveforms

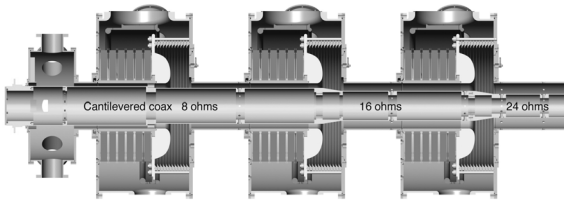

Fig. 8c. Induction Adder cross section

4. Operating Points in IVAs

The vacuum coax transmission line, which threads the induction cavities, supports the current and voltage, which ultimately drives the load. The physical understanding of magnetically insulated lines has been an active area of research for well over three decades [16, 17]. In a MITL the cathode electric field exceeds the threshold for electron emission (~200 kV/cm). The transverse magnetic field generated by the current flowing in the conductors is sufficient to keep the electrons from crossing the A-K gap (i.e. the electron flow is insulated) and power can be delivered efficiently to the load. The presence of electron flow causes the MITL operating impedance to be a non-linear function of the voltage and vacuum impedance, usually close to the minimum current condition for one dimensional laminar flow theory (Fig. 9) [16, 18].

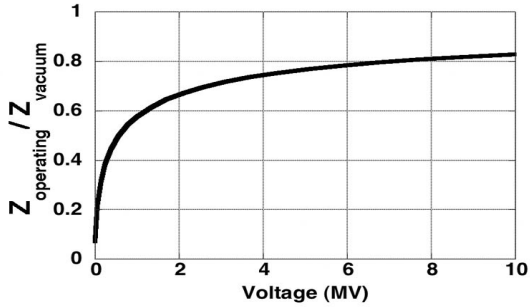

Fig. 9. Normalized MITL operating impedance for line-limited operation

It is important to note that, unlike a conventional transmission line where a miss-matched load induces a linear transformation in load voltage and current, a MITL will shed any excess current from an over-matched load with no voltage gain. A MITL responds to an undermatched load in a non-linear manner (discussed below). Since each cell adds voltage to the MITL stalk, the operating impedance increases along the adder. Accelerators are conventionally designed by choosing the desired output voltage and impedance, then dividing each by the number of induction cavities to obtain the cell voltage and matched increment in MITL impedance. The MITL geometry is then obtained by applying the model of Fig. 9.

RITS is an example of such a design. The increment in operating impedance per cell is 8.5 Ohms. At the matched 26 Ohm load output level the operating parameters 4 MV and 155 kA [19]. The vacuum electron current fraction increases with voltage, about half the total for RITS. This matched configuration provides the largest output power, but does not optimize the radiographic load parameters, as only the cathode current is used by high intensity diodes.

To optimize the load parameters, a different approach has been undertaken. A mismatched MITL was developed raising the impedance step from 8.5 Ohms to 14.25 Ohms, thereby increasing the 1.4 MV cell voltage to 1.75 MV to create a matched 5.25 MV, 120 kA output pulse. The corresponding vacuum and cathode currents are 65 kA and 55 kA respectively. This higher impedance MITL was then undermatched by the unchanged diode load impedance, creating a re-trapping wave which converts a significant portion of the vacuum flow electron current to cathode current. The distribution of current between the vacuum electron flow and the cathode conduction behind the re-trapping wave is obtained from one dimensional laminar flow theory (Fig. 10).

The vacuum electron current is seen to be re-trapped with only a minimal decrease in load voltage.

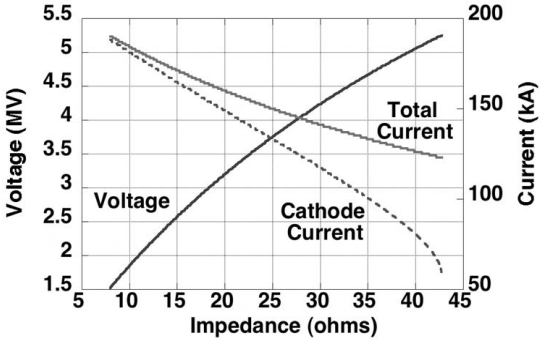

Fig. 10. High impedance RITS MITL predictions

For example, a 40 Ohm load produces a re-trapping wave in which the voltage is 5 MV, the vacuum electron current is 43 kA, and the boundary current is 84 kA. The useful cathode current is thus increased by 45% with only a 5% decrease in voltage. Comparing to the original MITL, a 30 Ohm load replicates the earlier 4 MV potential but with 120 kA of cathode current, a 60% increase in the useful radiographic power at the same voltage from the same accelerator. This analysis has been validated by both particle-in-cell simulations and experimental measurements (Fig. 11) [20, 21].

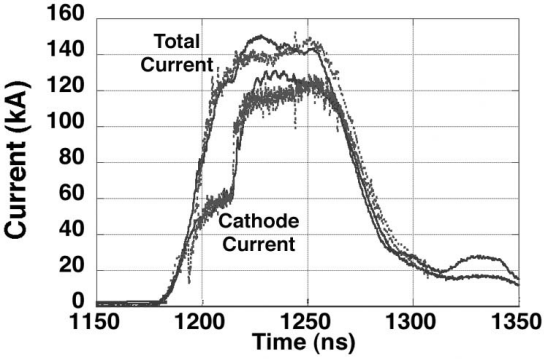

Fig. 11. PIC and Experimental data of a 6-cm blade load on RITS. Both the magnetic insulation wave and the re-trapping wave (jump in cathode current at ~ 1212 ns) are evident in the data and the simulation. The calculated re-trapping wave velocity is approximately 0.4 c, in agreement with the experimental data

This design approach miss-matching the IVA to the MITL to the diode load offers a new perspective and opportunities to create more flexible and efficient radiographic source accelerators.

5. Flexible Driver Operation

The ability to accurately predict the operating parameters of a miss-matched induction adder, MITL, and load enables the design of a flexible accelerator capable of driving a variety of diode loads. This is important both in the research phase of radiographic x-ray source investigations and possibly later in the deployment of a single system capable of providing a variety of radiation environments. The radiographic diode loads are designed to meet different voltage, dose, and spot size requirements, and represent a diverse suite of load impedances. The conventional approach has been to discard the MITL vacuum electron flow and design the accelerator cathode conduction current and voltage to match a particular diode. The recent advances discussed above show that this electron flow can be re-captured and converted to useful cathode conduction current, suggesting a different approach, which better utilizes the accelerator power pulse.

Figure 12 traces the retrapping load line for a hypothetical ten-cavity IVA accelerator, again in the context of the different diode requirements. For the following discussion the accelerator is assumed to be operated at identical full power configuration, irrespective of the load terminating the MITL. A very high impedance load such as the paraxial will absorb the 35 kA it is capable of reliably focusing. This is an overmatch to the accelerator, so the voltage will be 15 MV and the excess current will be shunted by the MITL before the diode inductance.

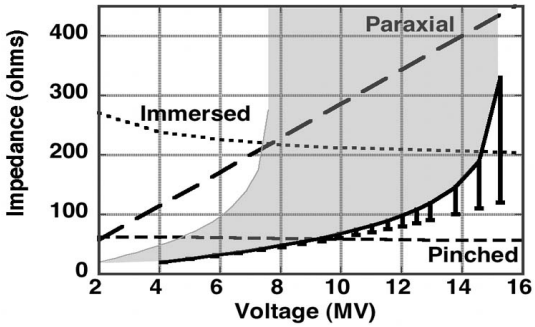

Fig. 12. Retrapping load line for a 10 Ohm, 1.4 MV PFL driving ten 12-Ohm MITL steps. Sheath flow is shown by the error bars on the load line. Shaded region is the accessible load operating regime

A magnetically immersed diode at 200 Ohms will slightly undermatch the output MITL, pulling down the voltage to 14.5 MV but coupling half the initial sheath flow into useful cathode conduction current launched into the focused electron beam. A pinched diode at 50 Ohms will severely reduce the voltage to 9 MV, but will focus 165 kA into a radiographic source spot. The different voltages, currents, and beam temperatures for these three diodes all scale to produce in excess of 1000 rads measured a meter from the source. Clearly the IVA accelerator may be operated at reduced Marx charge with slight modifications to the various switch settings to obtain a similar shaped load line shifted left from the one shown. This creates a broad operating space (shaded region) for possible diode research and applications, all within a single IVA accelerator instead of the conventional need for several drivers at different operating points.

6. Conclusions

The ability to drive various impedance focused electron beam diode loads with a single Induction

Voltage Adder accelerator adds to the versatility of this technology. As advances in high brightness electron beam sources continue, an integrated parallel effort is underway to develop ever more compact and inexpensive IVA drivers and to provide flexible and adaptive infrastructures for the breadth of flash radiographic x-ray source needs.

References

[1] T.J. Goldsack, T.F. Bryant, P.F. Beech, S.G. Clough, G.M. Cooper, R. Davitt, R.D. Edwards, N. Kenna, J. McLean, A.G. Pearce, M.J. Phillips, K.P. Pullinger, D.J. Short, M.A. Sinclair, K.J. Thomas, J.R. Threadgold, M.C. Williamson, and K. Krushelnick, IEEE Trans. Plasma Sci. **30**, No. 1, 239–253 (2002).

[2] J. O'Malley, J. Maenchen, and G. Cooperstein, *in: Proc. 14th IEEE Int. Pulsed Power Conf.*, Dallas, TX, June 16–18, 2003, IEEE Cat. No. 03CH37472C, pp. 21–28.

[3] B.V. Oliver, P.F. Ottinger, T.C. Genoni, J.W. Schumer, S. Strasburg, S.B. Swanekamp, and G. Cooperstein, "Magnetically-Insulated Electron Flow with Ions with Application to the Rod-Pinch Diode", *Phys. Plasmas*, March 2004.

[4] G. Cooperstein, J.R. Boller, R.J. Commisso, D.D. Hinshelwood, D. Mosher, P.F. Ottinger, J.W. Schumer, S.J. Stephanakis, S.B. Swanekamp, B.V. Weber, and F.C. Young, Phys. Plasmas **8**, No. 10, 4618–4636 (2001).

[5] J.R. Smith, R. Carlson, R.D. Fulton, R. Atles, V. Carboni, J.R. Chavez, P. Corcoran, W.L. Coulter, J. Douglas, D. Droemer, W.A. Gibson, T.B. Helvin, D.J. Henderson, D.L. Johnson, J.E. Maenchen, C.V. Mitton, I. Molina, H. Nishimoto, E.C. Ormond, P.A. Ortega, R.J. Quicksilver, R.N. Ridlon, E.A. Rose, D.W. Scholfield, I. Smith, A.R. Valerio, and R. White, *in: Proc. 14th Int. Conf. on High-Power Particle Beams*, Albuquerque, NM, June 23–28, 2002, pp. 135–138.

[6] D.V. Rose, D.R. Welch, B.V. Oliver, R.E. Clark, D.L. Johnson, J.E. Maenchen, P.R. Menge, C.L. Olson, and D.C. Rovang, J. Appl. Phys. **91**, No. 5, 3328–3335 (2002).

[7] S.B. Swanekamp, G. Cooperstein, J.W. Schumer, D. Mosher, F.C. Young, P.F. Ottinger, and R.J. Commisso, "Evaluation of Self-Magnetically-Pinched Diodes up to 10 MV as High-Resolution Flash X-Ray Sources", IEEE Transactions on Plasma Science special issue on Pulsed-Power Science and Technology, Oct. 2004 (to be published).

[8] I. Crotch, J. Threadgold, M. Sinclair, and A. Pearce, *in: Proc. 14th IEEE Int. Pulsed Power Conf.*, Dallas, TX, June 16–18, 2003, IEEE Cat. No. 03CH37472C, pp. 507–509.

[9] T.W.L. Sanford, J.A. Halbleib, J.A. Poukey, A.L. Pregenzer, R.C. Pate, C.E. Heath, R. Mock, G.A. Mastin, D.C. Ghiglia, T.J. Roemer, P.W. Spence, and G.A. Proulx, J. Appl. Phys. **66**, No. 1, 10–22 (1989).

[10] D.R. Welch, D.V. Rose, B.V. Oliver, E. Schamiloglu, K. Hahn, and J.E. Maenchen, Physics of Plasmas, No. 2, 751–760 (2004).

[11] M.G. Mazarakis, J.W. Poukey, J.E. Maenchen, D.C. Rovang, P.R. Menge, D.L. Smith, J.A. Halbleib, S.R. Cordova, L. Bennett, K. Mikkelson, R. Pepping, W.A. Stygar, T.G. Trucano, D.R. Welch, T.J.T. Kwan, B.G. DeVolder, R.J. Kares, and C.M. Snell, Appl. Phys. Lett. **70**, 832 (1997).

[12] J.J. Ramirez, D.E. Hasti, J.P. Corley, J.W. Poukey, K.R. Prestwich, R.D. Genuario, H.N. Nishimoto, J.J. Fockler, I.D. Smith, P.D'A Champney, K.E. Nielsen, L.G. Schlitt, and P.W. Spence, *in: Proc. of the 5th IEEE Pulsed Power Conference*, June 10–12, 1985, Arlington, VA, IEEE Cat. No. 85CH2121-2, pp. 143–146.

[13] J.J. Ramirez, K.R. Prestwich, J.A. Alexander, J.P. Corley, G.J. Denison, C.W. Huddle, D.L. Johnson, R.C. Pate, G.J. Weber, E.L. Burgess, R.A. Hamil, J.W. Poukey, T.W.L. Sanford, L.O. Seamons, G.A. Zawadzkas, I.D. Smith, P.W. Spence, and L.G. Schlitt, *in: Proc. Beams 88* (Karlsruhe), p. 148.

[14] I.D. Smith, V.L. Bailey, J. Fockler, J.S. Gustwiller, D.L. Johnson, J.E. Maenchen, D.W. Droemer, IEEE Trans. on Plasma Sci. **28**, 1653–1659, 28 (2000).

[15] I. Smith, P. Corcoran, V. Carboni, V. Bailey, H. Kishi, D.L. Johnson, J. Maenchen, I. Molina, R. Carlson, R.D. Fulton, K. Hahn, J. Smith, D. Droemer, K. Thomas, M. Phillips, S. Croxon, R. Forgan, and I.D. Smith, *in: Proc. 14th IEEE Int. Pulsed Power Conf.*, Dallas, TX, June 16–18, 2003, IEEE Cat. No. 03CH37472C, pp. 371–378.

[16] J.M. Creedon, J. Appl. Phys. **46**, 2946 (1975).

[17] C.W. Mendel Jr., D.B. Seidel, and S.E. Rosenthal, Laser Part. Beams **1**, 311 (1983).

[18] M.Y. Wang, M.S. DiCapua, JAP **51**, 5610 (1980).

[19] D.L. Johnson, I. Smith, P. Corcoran, V. Bailey, J. Douglas, V. Carboni, I. Molina, S. Portillo, K. Hahn, E. Puetx, S. Cordova, D. Droemer, T. Guy, R. Gignac, F. Wilkins, and R. Woodring, *in: Proc. 14th IEEE Int. Pulsed Power Conf.*, Dallas, TX, June 16–18, 2003, IEEE Cat. No. 03CH37472C, pp. 379–382.

[20] V.L. Bailey, D.L. Johnson, P. Corcoran, I. Smith, J. Maenchen, I. Molina, K. Hahn, D. Rovang, S. Portillo, B.V. Oliver, D. Rose, D. Welch, D. Droemer, and T. Guy, *in: Proc. 14th IEEE Int. Pulsed Power Conf.*, Dallas, TX, June 16–18, 2003, IEEE Cat. No. 03CH37472C, pp. 399–402.

[21] S. Portillo, K. Hahn, J. Maenchen, I. Molina, S. Cordova, D.L. Johnson, D. Rose, B. Oliver, and D. Welch, *in: Proc. 14th IEEE Int. Pulsed Power Conf.*, Dallas, TX, June 16–18, 2003, IEEE Cat. No. 03CH37472C, pp. 879–882.